Wall-induced order in anisotropic Lennard-Jones fluid in a nanochannel

R.M. Hartkamp[1], A. Ghosh[2] and S. Luding[1]
[1)] Multiscale Mechanics, University of Twente, Enschede, The Netherlands
Phone: +3153-4894732, e-mail: r.m.hartkamp@utwente.nl
[2)] Soft Matter, University of Amsterdam, Amsterdam, The Netherlands

Abstract
Highly confined fluid or particle flows typically show strongly non-Newtonian behavior. In this study, the relation between the non-Newtonian behavior and the level of confinement is studied. Molecular dynamics simulations, in the canonical ensemble (i.e. the number of particles, volume and temperature are constant), are used to calculate various physical properties. Here we only present the density profile for different channel widths, showing the near wall structure and layering being additive.

1 Introduction

Over the past decades molecular dynamics simulations have become an important tool for the study of microscopic fluid properties. A channel geometry is often used to study the inhomogeneous behavior of strongly confined fluids [1, 2, 3, 4, 5]. However, our understanding of these non-Newtonian fluid problems is still very limited, while gaining a deeper insight into these systems is becoming increasingly important with the rise of microfluidic and nanofluidic applications, such as lab-on-a-chip devices [6]. Very similar phenomenology (i.e. layering, anisotropy) is observed in many particle systems [7, 8].

In this study liquid argon is confined between two flat walls with a normal in the *x*-direction (Figure 1). When an atom leaves the system in *y*- or *z*-direction, it re-enters at the opposite side due to periodic boundary conditions. Both walls consist of two layers of argon atoms (each layer containing 128 atoms) fixed in a face centered cubic (fcc) lattice. The fluid-wall interaction is equal to the fluid-fluid interaction and the number density of the system is $\rho = 0.8$ (corresponding to a volume fraction of $\varphi = 0.415$).

Physical quantities are nondimensionalized by using the length, energy and mass scales of liquid argon, which are $\sigma = 3.405 \times 10^{-10}$ m, $\varepsilon = 1.67 \times 10^{-21}$ J and $m = 6.626 \times 10^{-26}$ kg respectively. A constant body force f acts on the fluid in negative z-direction, causing it to flow. The mutual interaction of the neutral spherically symmetric argon atoms is modeled via a two-body Lennard-Jones (LJ) potential:

$$U(r) = 4\varepsilon\left((\sigma/r)^{12} - (\sigma/r)^{6}\right), \tag{1}$$

with r the distance between two atom centers. From the interaction potential, the force between two atoms can be calculated:

$$F(r) = -\frac{\partial U}{\partial r} = 24\frac{\varepsilon}{\sigma}\left(2(\sigma/r)^{13} - (\sigma/r)^{7}\right) - F(\sigma_c). \tag{2}$$

The force is truncated at $\sigma_c = 2.5\sigma$ in order to reduce calculation time, therefore $F(r \geq \sigma_c) = 0$, where the second term in Eq. (2) leads to a continuous force.

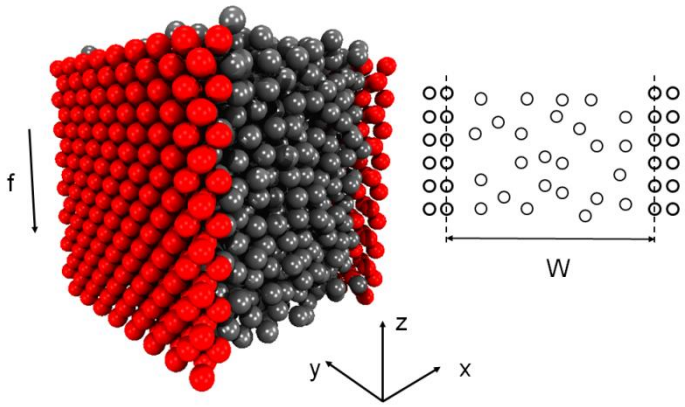

Figure 1: Liquid argon (grey, 1536 atoms) confined between solid argon walls (red, 512 atoms). The width of the channel is defined as shown on the right.

The natural time step, $\tau = (m\sigma^2/\varepsilon)^{1/2}$, is proportional to the period of oscillation about the potential minimum. For liquid argon, it is $\tau = 2.14 \times 10^{-12}$ s. From the positions, velocities and interatomic forces, other physical scalar or tensorial quantities can be calculated (e.g. shear rate, stress and viscosity) [9]. The position and momentum of every atom and the forces acting on them are used to calculate their position and velocity after an increment (Δt) in time via the Velocity Verlet algorithm, with a time step of $t = 0.001\tau$. The body force on the atoms leads to an acceleration of the fluid, while viscous effects retard the flow until a steady state is reached. Local thermostats near the walls keep the energy (and thus the temperature) constant in time ($T = 1.0$ for the simulations presented in this paper) [10, 11]. The steady-state simulation results are averaged over a period of time of the order of 1000 - 5000τ. Furthermore, spatial averaging is employed over the directions parallel to the solid walls, whereas, the x-direction (perpendicular to the solid walls) is divided into equally spaced bins of width $b = 0.083$.

2 Channel width dependence of the flow

Figure 2 shows a volume fraction profile in the channel for different channel widths. Each of the density profiles shows oscillatory behavior near the channel walls which decay exponentially away from the walls. The period and magnitude of the most apparent oscillations seems to be approximately identical for all three simulations (apart from statistical noise). In the largest system, a region of inhomogeneity can be identified near both walls as well as a bulk fluid-like (i.e. homogeneous) region in the center. Six distinct peaks are observed between each wall and the bulk fluid region of the channel (the increase in density very close to the wall is due to the wall atoms, the density of the fluid goes to zero there). Decreasing the system size, but keeping the density and temperature unchanged, the homogeneous region shrinks in size and finally disappears when the channel width becomes smaller than approximately 12σ. For narrower channels a region forms in the center where the oscillations in density, induced by both walls, interfere additively; the oscillatory behavior in this region becomes directly dependent on the system size.

It will be shown that by simply taking the density profile in the left and right inhomogeneous region of the largest system, one can predict the density profile in a system that is either larger or smaller.

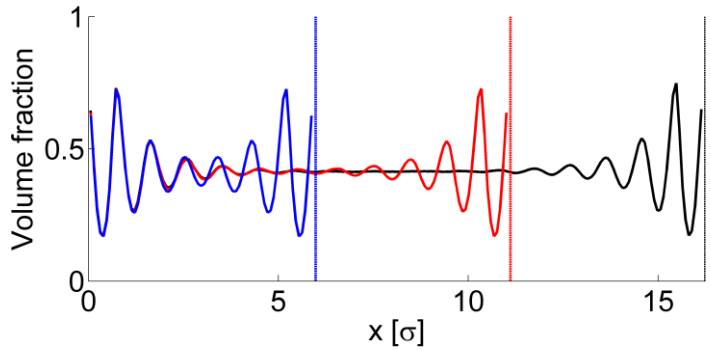

Figure 2: Density profile for 3 different channels with width W_1=5.985σ (blue), W_2=11.115σ (red) and W_3=16.245σ (black). The vertical lines represent the location of the right wall for that system.

3 Results & discussion

Consider the density profile in the left and right half of a channel that is wider than twice the inhomogeneous region (a channel width of 16.245σ is used here) and shift these towards each other until a channel of width 11.115σ is realized. The deviations from the average density are then just summed up. In Figure 3, the constructed profile is compared to the result of a molecular dynamics simulation.

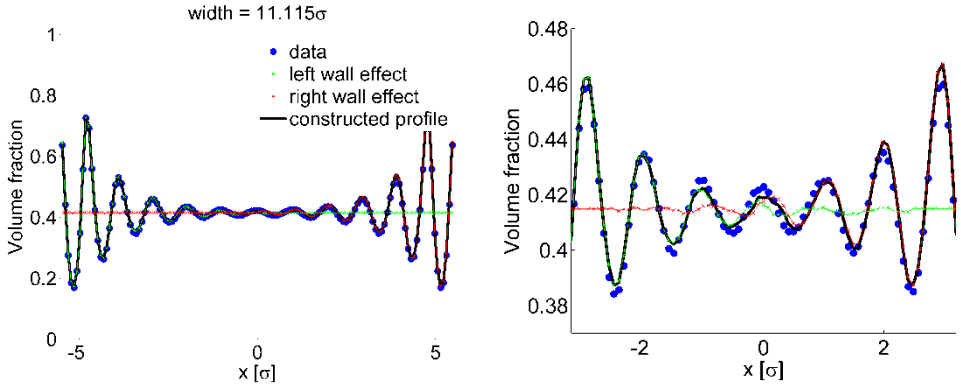

Figure 3: (Left) Comparison of a constructed density profile and the data of a molecular dynamics simulation for a channel of width W_2=11.115σ. (Right) Close-up of the center of the channel.

Figure 3 confirms that the interference of the oscillations is only significant in the region that is within 6σ distance from both walls and that the oscillations can be summed up approximately.

In the system (W_2) shown in Figure 3, the region where the influence of both walls overlaps is small and in this region so is the amplitude of the oscillations. If we apply the same approach to a more narrow channel (W_1), where the overlapping region dominates the system (i.e. the density profile in the whole system is directly influenced by both walls), we see a great correspondence to the density profile that was obtained by a molecular dynamics simulation (Figure 4), in both the magnitude and period of the oscillations.

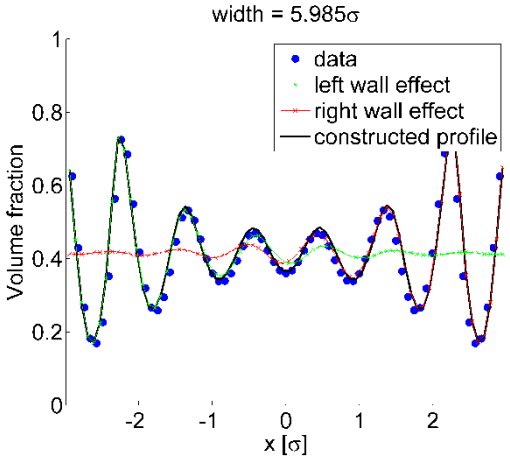

Figure 4: The comparison of a constructed density profile and the data of a molecular dynamics simulation for a channel of width W_1=5.985σ.

The approach that was presented here can be used to predict the oscillatory behavior in a channel without having to simulate the system explicitly. However, more extensive testing of the method is required, especially when the system width decreases below 5.985σ and for systems with other densities and temperatures. If a quantitative relation between the density profile and other physical properties can be found for this inhomogeneous channel flow, the method presented here could predict flow behavior of the fluid without the need of simulating every individual system width explicitly.

Acknowledgement
This work was financially supported by MicroNed grant 4-A-2.

References

[1] J. Koplik and J. R. Banavar. Molecular dynamics simulation of microscale poiseuille flow and moving contact lines. Phys. Rev. Lett., 60:1282, 1988.
[2] I. Bitsanis, T.K. Vanderlick, M. Tirrell and H.T Davis. A tractable molecular theory of flow in strongly inhomogeneous fluids. J. Chem. Phys., 89:3152, 1988.
[3] B.D. Todd and D.J. Evans. The heat flux vector for highly inhomogeneous non-equilibrium fluids in very narrow pores. J. Chem. Phys., 103:9804, 1995.
[4] K.P. Travis, B.D. Todd, and D.J. Evans. Departure from Navier-Stokes hydrodynamics in confined liquids. Phys. Rev. E, 55:4288, 1997.
[5] K.P. Travis and K.E. Gubbins. Poiseuille flow of Lennard-Jones fluids in narrow slit pores. J. Chem. Phys, 112:1984, 2000.
[6] A. van den Berg, W. Sparreboom and J.C.T. Eijkel. Principles and applications of nanofluidic transport. Nature Nanotechnology, 4:713, 2009.
[7] W. F. Van Gunsteren, H. J. C. Berendsen, J. P. M. Postma, A. DiNola, and J. R. Haak. Molecular Dynamics with Coupling to an external bath. J. Chem. Phys., 81:3684, 1984.
[8] A. Ghosh, R. Paredes and S. Luding. Poiseuille flow in a nanochannel - use of different thermostats. International Congress of Particle Technology, Nuremberg, Germany, pp. 1-4, CD Proceedings, 2007.
[9] R.M. Hartkamp, A. Ghosh and S. Luding, Anisotropy of a fluid confined in a nanochannel. 2010.
[10] M. Lätzel, S. Luding and H.J. Herrmann. Macroscopic material properties from quasi-static, microscopic simulations of a two-dimensional shear-cell. Granular Matter, 2:123, 2000.
[11] I. Bartos and I.M. Jánosi. Side pressure anomalies in 2D packings of frictionless spheres. Granular Matter, 9:81, 2007.